Analytica Chimica Acta 689 (2011) 47–51

Contents lists available at ScienceDirect

Analytica Chimica Acta

journal homepage: www.elsevier.com/locate/aca

In situ synthesis of thulium(III) hexacyanoferrate(II) nanoparticles and its application for glucose detection

Zuchao Meng, Jianbin Zheng*, Qinglin Sheng, Xiaohui Zheng

Institute of Analytical Science, Shaanxi Provincial Key Labortary of Electroanalytical Chemistry, Northwest University, Taibai Road, Xi'an, Shaanxi 710069, China

ARTICLE INFO

Article history:
Received 8 November 2010
Received in revised form
27 December 2010
Accepted 12 January 2011
Available online 19 January 2011

Keywords:
Biosensor
In situ synthesis
Thulium hexacyanoferrate
Glucose oxidase
Glucose

ABSTRACT

Thulium hexacyanoferrate (TmHCF) nanoparticles (NPs) were in situ synthesized within the chitosan film on the electrode surface by a biocatalyzed reaction. The properties of the obtained nanoparticles are characterized with scanning electron microscope (SEM) and energy-dispersive X-ray (EDX). The optimized conditions for the formation of TmHCF NPs were 16 mM $Fe(CN)_6^{3-}$ and 1.5 mM Tm^{3+} with an accumulation time of 20 min. Based on process of in situ synthesis of TmHCF NPs, a novel biosensor for glucose was designed, and there is a linear relationship between the current response of TmHCF NPs and glucose concentration. The linear range for glucose detection was 0.02–0.4 mM ($r = 0.9975$, $n = 5$) and 0.4–13.6 mM ($r = 0.9935$, $n = 10$) and the detection limit was 6 μM at a signal-to-noise ratio of 3.

1. Introduction

Owing to their unique and tunable chemical and physical properties, nanomaterials have attracted considerable interest in recent years [1–7]. However, their application is often limited for the aggregation of nanoparticles. In order to avoid this problem, some functional polymers with carboxylic acid, imine, amine or sulfonate groups can chelate metal ions. They are therefore widely used as nanoreactors for the synthesis of metal [8–11], semiconductors [12,13] and metal oxide/hydroxide NPs [14,15]. Such an in situ synthetic methodology can avoid nanoparticle aggregates, control the size and density of nanoparticles and form unique hybrid structures. This method consists of two steps in general: immobilizing metal ions or their complexes to suitable substrates by electrostatic or ion exchange reaction, etc., then converting metal ions or their complexes to metallic states with chemical or photochemical reductions, etc.

At present, biocatalyzed synthesis of nanoparticles is a new and attractive field. Generally, the biocatalytic precipitation of an insoluble product on electronic transducers was used as a general amplification route for the sensing and recognition of events by layered biomaterial sensing interfaces, such as enzyme-based electrodes, immunosensors and DNA sensors. Li et al. [16] utilized biological catalytic reaction to realize the enlargement of Au-NPs. Chu et al. [17] used ALP to catalyze the substrate into ascorbic acid that reduced silver ions to metal silver. Wang [18] and Arribas [19] described different biometallization routes for the formation of cupric-ferrocyanide nanoparticles. Kumar et al. [20] reported the synthesis of bimetallic Au–Ag alloy nanoparticles using a eukaryotic microorganism. Moreover, previous studies have confirmed that an amplified signal can be achieved for the sensing and recognition of events.

In this paper, we prepare TmHCF NPs based on an in situ synthesis method. Also, according to the relationship of current response of TmHCF NPs and glucose concentration, a novel biosensor is designed. Chitosan (CHIT) as a biocompatible polymer can chelate metal ions by its amine function [21,22]. After Tm^{3+} ions were chelated, ferrocyanides are produced by the enzymatic reaction. Then TmHCF NPs can be formed within the CHIT film. After being optimized, the proposed biosensor is used for the determination of glucose. Herein, the role of TmHCF NPs for the detection of glucose is electronic transducers that use the enzymatic recognition events for glucose sensing. Such in situ synthesis based on biocatalytic reaction provides a general platform for the preparation of nanoparticles and the design of novel biosensors.

2. Experimental

2.1. Reagents

Glucose oxidase (GOx) (E.C.1.1.3.4, 182 U/mg, Type X-S from *Aspergillus niger*), β-D(+)-glucose, potassium hexacyanoferrate (II),

* Corresponding author. Tel.: +86 29 88302077; fax: +86 29 88303448.
E-mail addresses: zhengjb@nwu.edu.cn, zcmeng6@163.com (J. Zheng).

0003-2670/$ – see front matter © 2011 Elsevier B.V. All rights reserved.
doi:10.1016/j.aca.2011.01.028

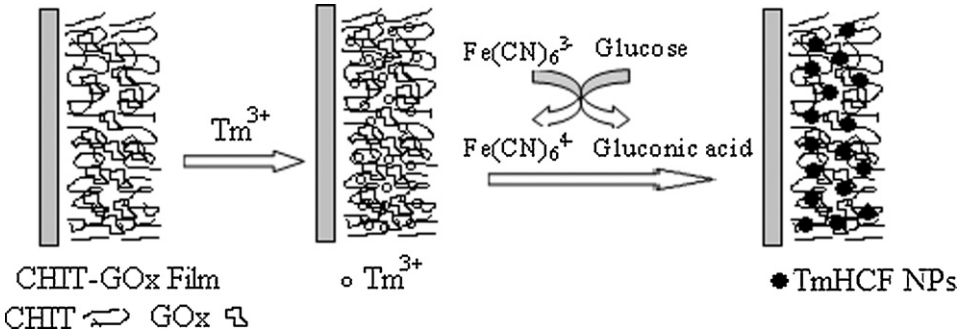

Scheme 1. Mechanism of GOx-induced formation of TmHCF NPs.

potassium hexacyaniferrate (III), thulium chloride hexahydrate (99.9%) and KCl were of analytical grades and used without further purification. All electrochemical experiments were conducted in 0.5 M KCl solution unless otherwise specified.

2.2. Apparatus

A Model CHI660A Electrochemistry Workstation (Chenhua Instruments, Shanghai, China) was employed for all the electrochemical techniques. A three-electrode system was used, where a standard saturated calomel electrode (SCE) served as the reference electrode, a platinum wire electrode as the auxiliary electrode, and the TmHCF–CHIT modified GC electrode as the working electrode. All the electrochemical experiments were conducted at room temperature ($26 \pm 2\,^{\circ}C$). Scanning electron microscopic (SEM) measurements were carried out on a scanning electron microscope (JEOL JSM - 6700 F) at 15 kV. Energy-dispersive X-ray (EDX) analysis was also performed during the SEM measurements.

2.3. Preparation of GOx–CHIT biocomposite modified electrode

A 1.0 wt% CHIT solution was prepared by dissolving certain amounts of CHIT into a 0.5 wt% acetic acid (HAc) and then was stored at $4\,^{\circ}C$. Prior to use, a bare glassy carbon electrode was polished with 0.3 and 0.05 μm aluminum oxide slurries and was rinsed with water, and then ultrasonicated in ethanol and ultrapure water respectively. The concentrations of GOx and CHIT were optimized in control experiments to obtain good current responses of GOx–CHIT-modified GCE. GOx stock solutions were prepared in 0.05 M phosphate buffer at pH 7.0. Typically, 5 μL of the mixture containing 2.0 mg mL^{-1} GOx and 3.0 mg mL^{-1} CHIT was spread evenly on the pretreated GCE surface. The resulting electrodes were

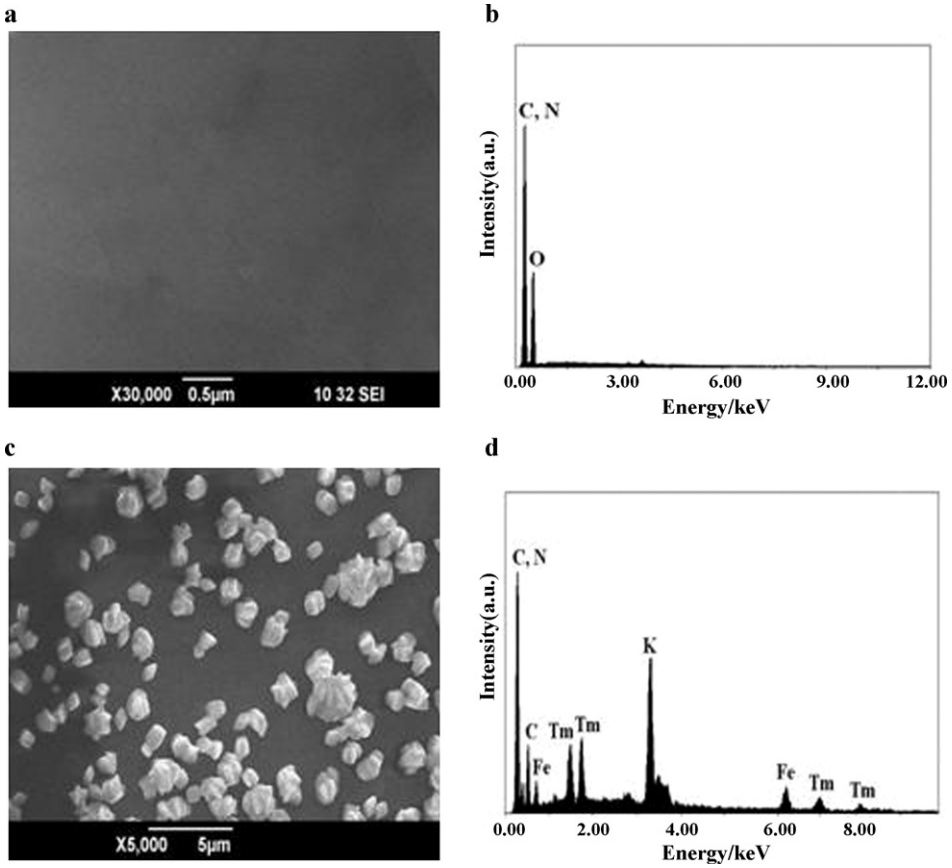

Fig. 1. (a) SEM images of GOx–CHIT composite film. (b) EDX analysis of GOx–CHIT composite film. (c) SEM images of TmHCF NPs in the CHIT film. (d) EDX analysis of TmHCF–CHIT composite film

dried at room temperature. Without use, the electrodes were stored at 4 °C in a refrigerator.

2.4. Experimental procedures

Cyclic voltammograms were obtained in the 0.5 M KCl solution. Electrochemical impedance spectroscopy (EIS) measurements were carried out in the 0.1 M $K_3Fe(CN)_6/K_4Fe(CN)_6$ (1:1) solution containing 0.5 M KCl. The AC voltage amplitude was 5 mV and the voltage frequency range was from 10 kHz to 0.1 Hz.

For the synthesis of TmHCF NPs, the CHIT–GOx/GC electrode was placed in a stirred 0.5 M KCl solution containing Tm^{3+} and $Fe(CN)_6^{3-}$ for a selected time. For the current response of TmHCF NPs generated by enzymatic reaction, the working electrode was placed in a blank 0.5 M KCl and recorded by square-wave voltammograms (SWVs). If not stated otherwise, SWV was conducted with the frequency of 10 Hz, potential step of 5 mV and pulse amplitude of 25 mV.

3. Results and discussion

3.1. Characterization of the biocatalytically induced TmHCF NPs

A possible process for the formation of TmHCF NPs in the CHIT films was shown in Scheme 1. First, Tm^{3+} ions were chelated by the amine group of CHIT. Then, when glucose was added to the solution, $Fe(CN)_6^{3-}$, severed as the electron acceptor, was reduced to $Fe(CN)_6^{4-}$ during the enzymatic reaction. By the electrostatic attraction between Tm^{3+} and $Fe(CN)_6^{4-}$ ions, TmHCF NPs were formed in the film.

Previous studies have shown that competitive adsorption and desorption exist between CHIT and metal ions under different experimental conditions. When the solution pH is more than 6, the competitive adsorption process is superior. The adsorption of metal ions by CHIT can reach more than 50%. Contrarily, when the solution pH is less than 6, the amino group of CHIT will combine H^+ to form $-NH_3^+$, leading to the decrease of chance for M^{3+} complex with CHIT [23]. Since the chelated Tm^{3+} was limited in the definite region of CHIT matrix, the formed particles were with a small size and were not liable to aggregate. Thus, a pH 7 value was selected as the optimum condition.

The presence of the TmHCF NPs was supported by SEM and EDX analyses. Before the enzymatic reaction, nothing could be observed on the electrode surface (Fig. 1a). The major elements of C and O could be seen on EDX spectrum of the electrode surface (Fig. 1b). After the enzymatic reaction, TmHCF NPs could be seen clearly in the CHIT film (Fig. 1c). Amplified image of TmHCF NPs showed that the structure of the generated TmHCF NPs was flake. That is, the generated flake TmHCF NPs clustered on the electrode surface. The average size of TmHCF NPs was 400 nm and distributed uniformly on the surface of the CHIT film. The EDX spectrum (Fig. 1d) showed the presence of Fe and Tm with an atomic ratio of 1:1. The result demonstrated that TmHCF NPs were successfully synthesized in the CHIT film.

3.2. EIS of the modifying process

EIS is a powerful tool for studying the interface properties of surface-modified electrodes [24,25]. The typical impedance spectrum (presented in the form of the Nyquist plot) includes a semicircle portion at higher frequencies corresponding to the electron-transfer-limited process and a linear part at a lower frequency range representing the diffusion limited process. The diameter of the respective semicircular element corresponds to the electron-transfer resistance (R_{et}) at the electrode surface. Fig. 2 shows the Nyquist plot of the differently modified electrodes in

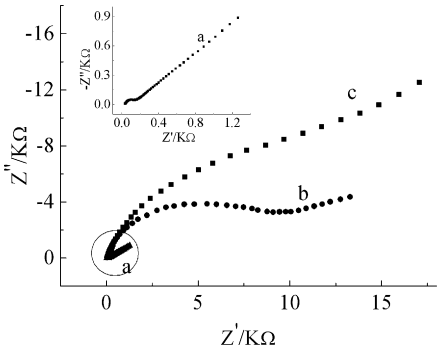

Fig. 2. EIS of (a) bare GC electrode, (b) GOx–CHIT/GC electrode, and (c) TmHCF–CHIT/GC electrode, in 0.5 mM $K_4[Fe(CN)_6]/K_3[Fe(CN)_6]$ solution containing 0.1 M KCl.

0.5 mM $Fe(CN)_6^{3-/4-}$ solution containing 0.1 M KCl. An almost straight line was observed for the bare GC electrode (R_{et} = 99 Ω) (curve a), which was the typical characteristic of a mass diffusion controlled electron transfer process. After being modified with GOx–CHIT film on the electrode surface (curve b), the R_{et} was increased to be 6345 Ω, indicating that GOx–CHIT film acted as a barrier for the electron transfer. After enzymatic reaction, a decrease in the interfacial resistance could be observed (curve c) (R_{et} = 6298 Ω), which might be attributed to the good conductive properties of TmHCF NPs.

3.3. Electrochemical properties of TmHCF

Before and after the in situ synthesis of TmHCF, the cyclic voltammograms of the modified electrode were recorded. From Fig. 3, it could be seen that curve b had a pair of well-defined redox peaks (peaks potential: E_{pa} = 0.309 V, E_{pc} = 0.099 V). Correspondingly, no electrochemical signal on the GOx–CHIT/GC electrode could be observed. It was therefore reasonable to conclude that TmHCF NPs were formed on the CHIT/GC electrode successfully.

The electrode reaction of TmHCF was similar to those reported about other hexcyanoferrate [26–29], and could be described as the following:

$$KTmFe^{II}(CN)_6 \rightarrow TmFe^{III}(CN)_6 + K^+ + e^- \quad (1)$$

3.4. Optimum conditions for the formation of TmHCF NPs

The optimum conditions for the formation of TmHCF NPs under biocatalytic conditions were examined by SWV. Accumulation time, $Fe(CN)_6^{3-}$ concentration, Tm^{3+} concentration were three major factors influencing the formation of TmHCF NPs (Fig. 4). Fig. 4a showed that the peak currents were increased with the accumulation time and the peak currents kept steady after 20 min.

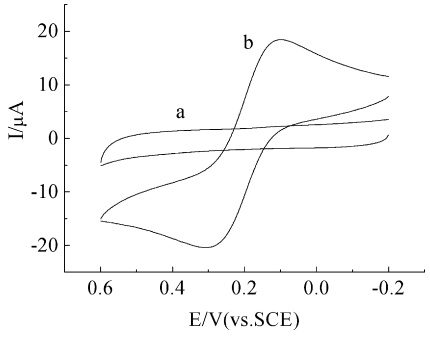

Fig. 3. Cyclic voltammograms of a GOx–CHIT/GC electrode (a) and TmHCF–CHIT/GC electrode (b) in 0.1 M KCl solution at a scan rate of 100 mV s^{-1}.

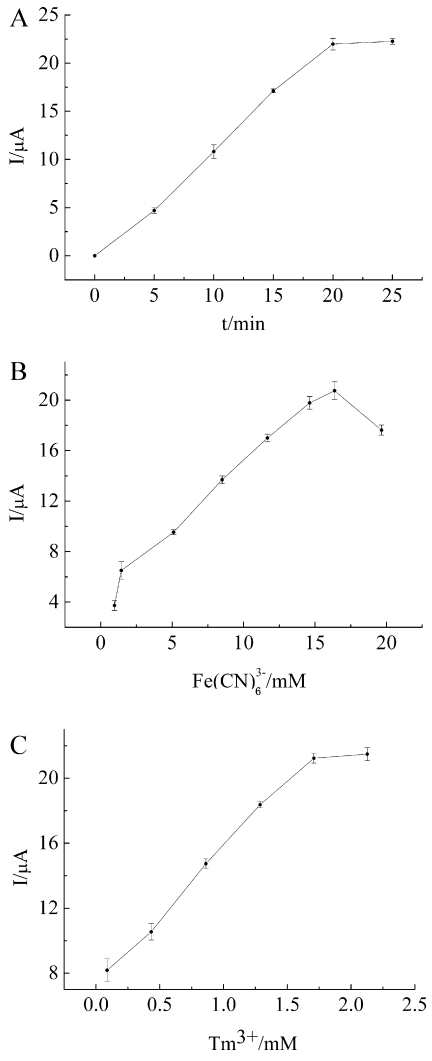

Fig. 4. Effect of accumulation time (a), $Fe(CN)_6^{3-}$ concentration (b), Tm^{3+} concentration (c) on the formation of TmHCF NPs. Reaction conditions: (a) a stirred 0.5 M KCl solution containing 16 mM $Fe(CN)_6^{3-}$ and 1.5 mM Tm^{3+}; (b) a stirred 0.5 M KCl solution containing 1.5 mM Tm^{3+} and different concentrations of $Fe(CN)_6^{3-}$ for 20 min; (c) a stirred 0.5 M KCl solution containing 16 mM $Fe(CN)_6^{3-}$ and different concentrations of Tm^{3+} for 20 min. The glucose concentration for the investigation of different components of the enzymatic reaction was 0.8 mM. The error bars represent the standard deviations of three measurements.

Therefore, we chose 20 min as the accumulation time. From Fig. 4b, it can be seen that the peak current was the highest when $Fe(CN)_6^{3-}$ concentration was about 16 mM, after which the peak current decreased. This may be ascribed to the electrostatic attraction between $Fe(CN)_6^{3-}$ and Tm^{3+} that leads to the decrease of Tm^{3+} being chelated by the amine group of CHIT. So we set $Fe(CN)_6^{3-}$ concentration as 16 mM. Fig. 4c shows that after Tm^{3+} concentration was 1.5 mM, the peak current kept steady. Therefore, we set Tm^{3+} concentration as 1.5 mM.

3.5. Square-wave voltammetric application for the determination of glucose

With the increase of glucose concentration, the current response of the generated TmHCF NPs on the electrode surface was also increased. And within a certain range, the current response showed a linear relationship with the glucose concentration. So the TmHCF NPs could be used as a biosensor for glucose detection. Fig. 5 shows SWVs for increasing concentration of glucose over the 0.02–13.6 mM range. From the inset graph in Fig. 5, it can be

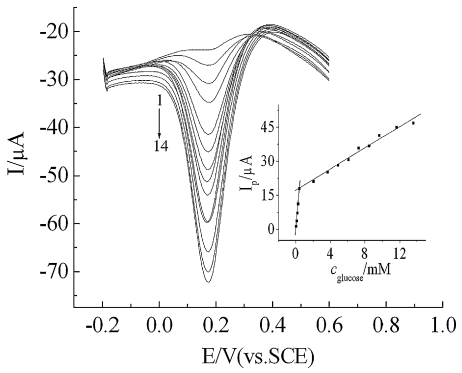

Fig. 5. SWVs of TmHCF NPs for an increasing concentration of glucose. Glucose concentration ranges 0.02–13.6 mM. Inset graph: calibration plot of peak current *vs.* glucose concentration. Reaction solution: a stirred 0.5 M KCl solution containing 1.5 mM Tm^{3+}, 16 mM $Fe(CN)_6^{3-}$, and different concentrations of glucose.

seen that the linear relationship between current response and glucose concentration was 0.02–0.4 mM ($r = 0.9975$, $n = 5$) and 0.4–13.6 mM ($r = 0.9935$, $n = 10$). The sensitivity of the biosensor was 2.35 μA mM^{-1} and 44.51 μA mM^{-1}. The detection limit was 6 μM at a signal-to-noise ratio of 3, which was significantly lower than previous reports using mesocellular silica–carbon nanocomposite foam (34 μM) [30], graphene/AuNPs/chitosan (180 μM) [31], silica sol–gel/GOD/CNTs (50 μM) [32] and Nafion–Pd–GOD–CNTs (150 μM) [33] as immobilization materials. The lower detection limit can be attributed to the generation of the TmHCF NPs under biocatalytic conditions that can increase the catalytically electroactive surface area and thus improve the biocompatible microenvironment to maintain the activity of the enzyme.

The apparent Michaelis–Menten constant K_m is generally used to evaluate the biological activity of the enzymatic reaction. And it can be calculated according to the Michaelis–Menten equation [34]:

$$\frac{1}{I_{ss}} = \frac{1}{I_{max}} - \frac{K_m}{I_{max} C_s} \quad (2)$$

where I_{ss} is the steady-state current, I_{max} is the maximum current measured under saturated substrate conditions, C refers to the glucose concentration, K_m is the apparent Michaelis–Menten constant, and I_{max} is the intercept on the current axis. Based on the experimental data, K_m was calculated to be 4.7 mM, which was smaller than the reported K_m of free GOx [35–37]. The smaller K_m value means that the immobilized GOx possess higher enzymatic activity and the proposed electrode exhibits a higher affinity to glucose.

3.6. Interference study on the determination of glucose

The selectivity of the glucose biosensor was examined in the presence of ascorbic acid and uric acid with glucose concentration at 0.4 mM. While uric acid concentration was 0.1 mM, the current increased by 0.2%. In the presence of ascorbic acid (0.1 mM), the current decreased by 0.2%. The results indicated that the biosensor had good anti-interferent ability for glucose detection.

3.7. Repeatability and stability of the biosensor

The repeatability and storage stability of the proposed biosensor have also been studied. The relative standard deviation (RSD) of five successive measurements to 1.0 mM glucose was 2.7%. The repeatability of six biosensors, made independently, was estimated with the RSD of 3.5% for the detection of 1.0 mM glucose. The biosensor was dried at 4 °C and it remained about 85% of its original sensitivity after 10 days.

Table 1
Determination of glucose in human plasma samples by the proposed biosensor.

Sample no.	Found (mM)	Added (mM)	Found (mM)	Recovery (%)
1	5.46	1.50	6.94	98.7
2	5.51	2.50	8.10	103.6
3	5.48	3.00	8.52	101.3

3.8. Application for the glucose determination

The determination of glucose levels in human plasma was performed by the proposed biosensor. The complete blood sample was prepared through immediate centrifugation for 10 min at 4 °C to obtain the plasma sample. After that, the sample solutions were prepared by diluting the corresponding plasma sample with a buffer solution to the original volume and used for bioassay. At first, the GOx/CHIT film modified GCE was immersed in a stirred 0.5 M KCl solution containing 1.5 mM Tm^{3+} and 16.0 mM $Fe(CN)_6^{3-}$. Then, 1.0 mL of sample solution was added. After incubation in the above solution for 20 min, the electrode was washed with water and transferred into a 0.5 M KCl solution, after which SWV signals were recorded. The measureable results were listed in Table 1. The average glucose level in human plasma was found to be 5.5 mM. The recoveries for the determination of glucose were between 98.7% and 103.6% for three times determination.

4. Conclusions

The present work demonstrates a new method for the formation TmHCF NPs in situ by biocatalyzed reaction on glass carbon electrodes. Beneficially, the method is simple and easy to control. According to the response current generated from TmHCF NPs, the glucose biosensor can be fabricated. The biosensor showed good conductivity, stability and wide linear concentration ranges towards glucose detection. It is expected that the present technique can be used for the design of sensitive and selective electrochemical biosensors within other bio-systems.

Acknowledgements

The authors appreciate the financial support from the National Natural Science Foundation of China (No. 20875076), the Science Foundation of Northwest University (No. NF0902), the Shaanxi Province “13115” Scientific and Technological Innovation Project (No. 2007ZDKG-70) and the NWU Doctorate Dissertation of Excellence Funds (No. 08YYB06).

References

[1] V.L. Colvin, M.C. Schlamp, A.P. Alivisatos, Nature 370 (1994) 354–357.
[2] K. Aslan, S.N. Malyn, C.D. Geddes, J. Am. Chem. Soc. 128 (2006) 13372–13373.
[3] S.J. Guo, S.J. Dong, Trends Anal. Chem. 28 (2009) 96–109.
[4] M.T. Sulak, Ö. Gökdoğan, A. Gülce, Biosens. Bioelectron. 21 (2006) 1719–1726.
[5] Q.L. Sheng, J.B. Zheng, Biosens. Bioelectron. 24 (2009) 1621–1628.
[6] L.D. Feng, M.M. Gu, Y.L. Yang, G.X. Liang, J.R. Zhang, J.J. Zhu, J. Phys. Chem. C 113 (2009) 8743–8749.
[7] L.D. Feng, J.M. Shen, X.H. Li, J.J. Zhu, J. Phys. Chem. C 113 (2009) 7617–7623.
[8] N. Singh, P.K. Khanna, Mater. Chem. Phys. 101 (2007) 367–372.
[9] J.J. Li, Y.P. Chen, Y.J. Yin, F.L. Yao, K.D. Yao, Biomaterials 28 (2007) 781–790.
[10] N.E. Kotel'nikova, E.L. Lysenko, R. Serimaa, K. Pirkkalainen, U. Vainio, V.K. Lavrent'ev, D.A. Medvedeva, A.L. Shakhmin, N.N. Saprykina, N.P. Novoselov, Polym. Sci. Ser. A 50 (2008) 51–57.
[11] Y.Q. Liu, M.L. Yang, Z.K. Zheng, B.L. Zhang, Electrochim. Acta 51 (2005) 605–610.
[12] A.V. Firth, S.W. Haggata, P.K. Khanna, S.J. Williams, J.W. Allen, S.W. Magennis, I.D.W. Samuel, D.J. Cole-Hamilton, J. Lumin. 109 (2004) 163–172.
[13] M. Zhang, M. Drechsler, A.H.E. Müller, Chem. Mater. 16 (2004) 537–543.
[14] M.A. Morales, P.V. Finotelli, J.A.H. Coaquira, Mater. Sci. Eng. C 28 (2008) 253–257.
[15] W.S. Choi, H.Y. Koo, J.H. Park, D.Y. Kim, J. Am. Chem. Soc. 127 (2005) 16136–16142.
[16] N.D. Zhou, J. Wang, T. Chen, Z.G. Yu, G.X. Li, Anal. Chem. 78 (2006) 5227–5230.
[17] Y. Tan, X. Chu, G.L. Shen, R.Q. Yu, Anal. Biochem. 387 (2009) 82–86.
[18] J. Wang, A.S. Arribas, Small 2 (2006) 129–134.
[19] A.S. Arribas, T. Va′zquez, J. Wang, A. Mulchandani, W. Chen, Electrochem. Commun. 7 (2005) 1371–1374.
[20] S. Senapati, A. Ahmad, M.I. Khan, M. Sastry, R. Kumar, Small 1 (2005) 517–520.
[21] R. Khan, A. Kaushik, P.R. Solanki, A.A. Ansari, M.K. Pandey, B.D. Malhotra, Anal. Chim. Acta 616 (2008) 207–213.
[22] X.H. Wang, Y.M. Du, H. Liu, Carbohydr. Polym. 56 (2004) 21–26.
[23] M. Rhazi, J. Desbrières, A. Tolaimate, M. Rinaudo, P. Vottero, A. Alagui, M. El Meray, Eur. Polym. J. 38 (2002) 1523–1530.
[24] Q.L. Sheng, K. Luo, L. Li, J.B. Zheng, Bioelectrochemistry 74 (2009) 246–253.
[25] R.F. Gao, X.D. Shangguan, G.J. Qiao, J.B. Zheng, Electroanalysis 20 (2008) 2537–2542.
[26] V. Malev, V. Kondratiev, V. Zigel, V. Kurdakova, Solid State Ionics 169 (2004) 95–104.
[27] S.Q. Liu, H.Y. Chen, J. Electroanal. Chem. 528 (2002) 190–195.
[28] P. Wu, C.X. Cai, J. Electroanal. Chem. 576 (2005) 49–56.
[29] P. Wang, Y. Yuan, X.Y. Jing, G.Y. Zhu, Talanta 53 (2001) 863–869.
[30] S. Wu, H. Ju, Y. Liu, Adv. Funct. Mater. 17 (2007) 585–592.
[31] C.S. Shan, H.F. Yang, D.X. Han, Q.X. Zhang, A. Ivaska, L. Niu, Biosens. Bioelectron. 25 (2010) 1070–1074.
[32] A. Salimi, R.G. Compton, R. Hallaj, Anal. Biochem. 333 (2004) 49–56.
[33] S.H. Lim, J. Wei, J. Lin, Q. Li, J.K. You, Biosens. Bioelectron. 20 (2005) 2341–2346.
[34] R.A. Kamin, G.S. Wilson, Anal. Chem. 52 (1980) 1198–1205.
[35] B.E.P. Swoboda, V. Massey, J. Biol. Chem. 240 (1965) 2209–2215.
[36] Y. Huang, W. Zhang, H. Xiao, G. Li, Biosens. Bioelectron. 21 (2005) 817–821.
[37] Y.Y. Wang, X.S. Wang, B.Y. Wu, Z.X. Zhao, F. Yin, S. Li, X. Qin, Q. Chen, Sens. Actuators B 130 (2008) 809–815.